Deflection Error Prediction and Minimization in 5-Axis Milling Operations of Thin-Walled Impeller Blades

Mohsen Soori (mohsen.soori@gmail.com)
Eastern Mediterranean University https://orcid.org/0000-0002-4358-7513
Mohammed Asmael
Eastern Mediterranean University: Dogu Akdeniz Universitesi

Original Article

Keywords: Deflection error, Impeller, 5-Axis CNC machine tools, Virtual machining

Posted Date: October 9th, 2020

DOI: https://doi.org/10.21203/rs.3.rs-87233/v1

Deflection Error Prediction and Minimization in 5-Axis Milling Operations of Thin-Walled Impeller Blades

Mohsen Soori *, Mohammed Asmael

Department of Mechanical Engineering, Eastern Mediterranean University, Famagusta, North Cyprus, Via Mersin 10, Turkey

* Corresponding author

E-mail addresses: mohsen.soori@gmail.com, mohsen.soori@emu.edu.tr (Mohsen Soori), mohammed.asmael@emu.edu.tr (Mohammed Asmael

Abstract:

To enhance accuracy as well as efficiency in process of machining operations, the virtual machining systems are developed. Free from surfaces of sophisticated parts such as turbine blades, airfoils, impellers, and aircraft components are produced by using the 5-axis CNC machine tools which can be analyzed and developed by using virtual machining systems. The machining operations of thin walled structures such as impeller blades are with deflection errors due to cutting forces and cutting temperatures. The flexibility of thin walled impeller blades can cause machining defects such as overcut or undercut. So, the desired accuracy in the machined impeller blades can be achieved by decreasing the deflection error in the machining operations. To minimize the deflection of machined impeller blades, optimized machining parameters can be obtained. An application of virtual machining system in predicting and minimizing the deflection errors of 5-Axis CNC machining operations of impeller blades is presented in the study to increase accuracy and efficiency in process of part production. The finite element analysis is applied to obtain the deflection error in machined impeller blades. In order to minimize the deflection error of impeller blades in the machining operations, the optimization methodology based on the Genetic algorithm is applied. The impeller is machined by using the 5-axis CNC machine tool in order to validate the developed virtual machining system in the study. Then, the machined impeller is measured by using the CMM machines to obtain the deflection error. As a result, the deflection error of in machining operations of impeller by using 5-Axis CNC machine tools can be decreased in order to enhance accuracy and efficiency of part manufacturing.

Keywords: Deflection error, Impeller, 5-Axis CNC machine tools, Virtual machining

1- Introduction

In order to increase accuracy in machining operations, virtual machining systems are recently applied to the process of part production using CNC machine tools. The systems can analyze the process of machining operations to be developed. To enhance efficiency in process of machining operations, applications of the virtual machining systems in optimizations of the machining process can be developed. Optimized parameters of machining operations can be obtained using optimization methodologies in order to decrease the deflection error in machining operations of thin walled components. So, developed methods of part production using machining operations can be presented using virtual machining systems in order to increase added values in produced parts.

The integral impeller and bladed disk are extensively used in different aircraft engines. The jet engine parts are produced with high level of accuracy and reliability regarding the safety concerns of aviation parts in order to present a good performances in working conditions. The application of the impeller in the HF-120 turbofan engine (GE-Honda) is shown in the figure 1 [1].

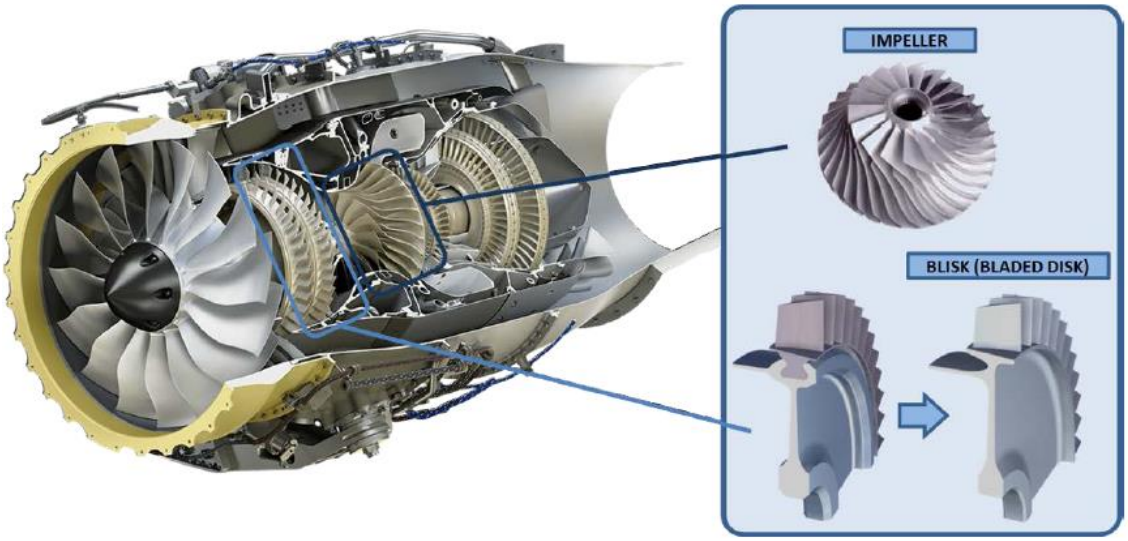

Fig. 1. Application of Blisk and impeller in the HF-120 turbofan engine (GE-Honda) [1].

The sophisticated parts with free form surfaces such as impeller blades are machined by using the -axis CNC machine tools. The machining operations using the 5-axis CNC machine tools are always with complexities and challenges which are studied in many research works. In machining operations of thin walled structures such as impeller blades, the deflection error is created due to the cutting forces and cutting temperature. The flexibility of thin walled impeller blades can cause machining defects such as overcut or undercut. So, the deflection error can create inaccuracy in machined parts which should be analyzed and decreased. The high accuracy requirement in machining operations of complex parts such as jet engine impeller blades is with complexities and challenges. As a result, the virtual machining system which can analyze and decrease the deflection error in machining operations of thin walled impellers can provide a key tool in terms of accuracy enhancement of machined impellers using 5-Axis CNC machine tools.

2- Review of research works in the deflection errors of thin walled machined parts

A framework for accuracy enhancement in milling operations of thin-walled narrow-vane turbine impeller of NiAl-based superalloy is presented by Zhao et al. [2] to increase accuracy and reliability of machined turbine impeller. In order to decrease the vibration and deformation in ball-end milling of thin-walled impeller blades, an optimization methodology for the cutting tool orientation is developed by Huang et al [3]. To increase accuracy in 5-axis machining operations of impeller blades, optimized strategy for finishing operations in the final step of the machining process is presented by Chaves-Jacob et al. [4]. The machining operations errors in 5-Axis adaptive flank milling of thin walled impeller blades is analyzed and decreased by Huang et al. [5] to develop the process of machining operations of flexible parts. To analyze an decrease the deflection error in milling thin-walled impeller blade, an advanced method to predict the deflection error is investigated by Liu et al. [6].

To reduce the deflection error in milling operation of flexible parts due to the cutting forces, the mathematical modelling of the thin-walled workpiece is investigated by Khandagale et al. [7]. An advanced method of deflection error prediction in peripheral milling of thin-walled workpieces is presented by Kang and Wang [8] in order to increase accuracy in machined parts. To decrease the deflection errors due to instability and deformation in the machined parts, the milling operations of light alloys with thin walled structures is studied by Del Sol et al. [9]. The effects of the cutting tool parameters such as tool helix angle to the accuracy and quality of machined parts is studied by Bolar and Joshi [10] in order to increase accuracy of machined parts by using the milling operations. Effects of machining parameters to the surface roughness and form errors in 4-axis milling of thin-walled free-form parts is studied by de Oliveira et al. [11]to reduce the deflection errors in the machined parts.

To simulate and analyze the cutting tool and workpiece deflection error in the machining operations of low rigidity thin walled parts, an advanced numerical modelling system is presented by Bolar and Joshi [12]. To compensate and decrease the deflection error in the flank milling operations of thin walled parts, an advanced cutting tool path optimization method is developed by Li and Zhu [13]. To increase surface quality and accuracy of machined impellers by using 5- Axis CNC machine tools, an advanced machining parameters optimization system is presented by Wang et al. [14]. An advanced machining parameter optimization system is investigated by Ratchev et al. [15] to enhance surface quality of machined thin walled parts by reducing the workpiece deflection errors. To compensate the strength loss due to the presence of the cut-out under bending operation, experimental investigation of buckling of wind turbine tower cylindrical shells with opening and stiffening is investigated by Dimopoulos and Gantes [16]. Structural efficiency of a wind turbine blade is studied by Buckney et al. [17] in order to improve designing process, minimizing weight and reducing the cost of wind energy.

To analyze and modify the machining operations in virtual environments, virtual machining systems and applications is presented by Soori et al. [18-21]. Virtual machining system and application is also presented by Altintas and Merdol [22] in order to obtain optimized condition of milling operations. In order to predict and minimize the deflection errors in five-axis milling operations of thin-walled parts such as impeller blades, an advanced methodology is proposed in the study. A virtual machining system is developed in the study to predict and minimize the deflection error of thin walled impeller blades by calculating the cutting forces as well as cutting temperatures at each position of cutting tool along machining paths. The Finite Element Analysis (FEM) is used to calculate the deflection error in the machined impeller. To minimize the deflection error, optimization technique based on the genetic algorithm is developed in order to obtain the optimized machining parameters. Experiment of machining operations of the impeller blade is carried out by using the 5-axis CNC machine tool in order to validate the effectiveness of the developed virtual machining system in the study. Then, to obtain the deflection error, the machined part is measured by using the CMM machines. As a result, accuracy as well as efficiency in process of impeller machining operations can be increased by applying the developed algorithm in the study. The method to calculate cutting forces in milling operations of thin walled parts and cutting temperatures are presented in the section 3 and 4 respectively. The deflection error of thin-wall workpiece in machining operations is analyzed in the section 5. The developed virtual machining system to predict and minimize the defection error is presented in the section 6. Finally, to validate the developed virtual machining system to minimize the deflection error of thin walled machined impeller blades, the section 7 is presented.

3- Cutting force model in milling operations of thin walled parts

To calculate the cutting forces in 5-axis machining operation of thin walled parts, the cutting force model developed by Li et al. [23] is implemented. The figure 2 [23] shows the basic structural movement of the end-mill operation which is described by two guiding curves during five-axis milling operations.

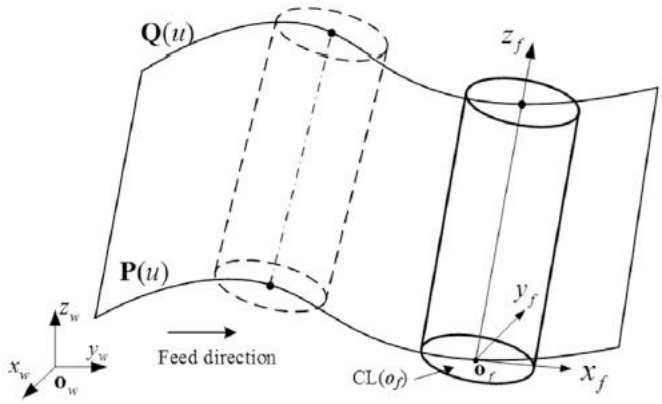

Fig. 2. General spatial motion of the end-mill in 5-Axis milling operation [23].

The two guided curves of $P(u)$ and $Q(u)$ are defined in order to simulate the cutting tool paths in the machining operations. As a result, cutter location of the (CL) can be described by using a moving feed coordinate as:

$$x_f = \frac{y_f \times A(u)}{\|y_f \times A(u)\|},\ y_f = \frac{A(u) \times \dot{p}(u)}{\|A(u) \times \dot{p}(u)\|}, z_f = A(u), \quad (1)$$

Where $\dot{p}(u)$ is the feed vector at the cutting tool tip which is due to the guiding curve $P(u)$. Moreover, x_f is described in the plane defined by the feed direction and axis vectors of cutting tool along machining paths and y_f is normal to this obtained plane. Also, $A(u)$ presents the unit vector along the cutting tool axis,

$$A(u) = \frac{Q(u) - P(u)}{\|Q(u) - P(u)\|} \quad (2)$$

The cutting tool in 5-Axis milling operations of thin walled parts is within cutting entry angle for i_{th} cutting element of cutting tool as is shown in the figure 3 [23].

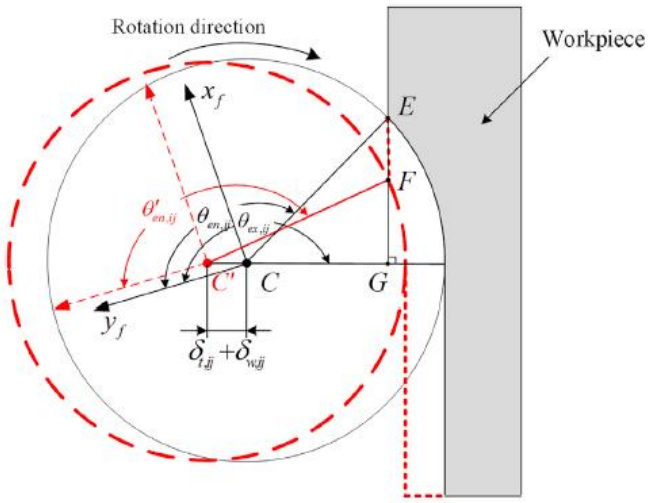

Fig. 3. The entry angle for the i_{th} cutting element of cutting tool during the five axis milling of thin walled workpiece [23].

The cutting entering angle can be presented as,

$$\theta'_{en,ij} = \theta_{ex,ij} - \text{acos}\left(\frac{\delta_{t,ij}+\delta_{w,ij}+R_{ij}.Cos(\theta_{ex,ij}-\theta_{en,ij})}{R_{ij}}\right) \quad (3)$$

Where $\theta_{en,ij}$ is the entry angle of the cutting tool along machining paths, $\delta_{t,ij}$ and $\delta_{w,ij}$ are the deflection errors of the cutting tool and workpiece for the normal direction of the i_{th} cutter element surface on the j_{th} flute of the cutting tool, respectively. Moreover, R_{ij} is the rotation radius of the i_{th}cutter element on the j_{th} flute of the cutting tool.
In five axis milling operations of the thin walled parts, the cutting tool orientation is changing continuously due to cutting tool paths on the free form surfaces and new angles and positions of flexible parts during machining operations. As a result, the cutter runout should be considered in terms of cutting forces calculation [23]. The figure 4 shows the instantaneous uncut chip thickness calculation by considering the cutter runout during the five axis milling operations of thin walled parts [23].

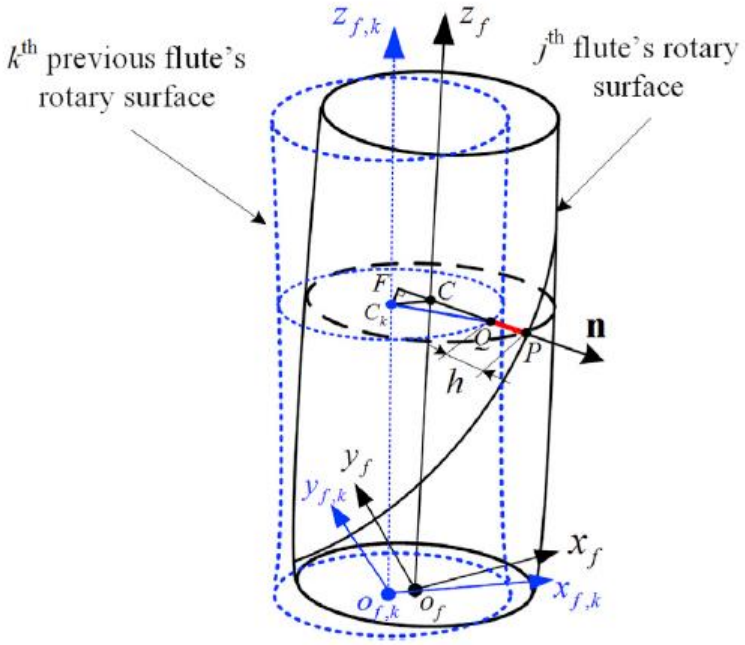

Fig. 4. The instantaneous uncut chip thickness calculation by considering the cutter runout during the five axis milling operations of thin walled parts [23].

As a result, the uncut chip thickness for the ith cutter element of the jth flute by considering the kth previous flute at angular position $\theta_{ij}$and cutter location u can be obtained as,

$$h_{ij,k}(\theta_{ij},u) \approx \frac{k.f_t}{\|\acute{p}(u)\|}\left(\acute{p}(u) + z_i\acute{z}_f(u)\right)n + R_{ij} - R_{i(j-K)} \quad (4)$$

Where,

$$n = \sin\theta_{ij}x_f(u) + \cos\theta_{ij}y_f(u) \quad (5)$$

Where R_{ij} is the rotation radius of the i_{th}cutter element on the j_{th} flute and f_t is the feed per tooth along machining paths. As a result, the applied cutting forces in the radial, tangential and axial directions of the ith axial disk element of the jth flute can be calculated in the differential format as follows,

$$F_{q,ij}(\theta_{ij},u) = g(\theta_{ij})\left[K_{qc}h_{ij}(\theta_{ij},u)b_i + K_{qe}.S_i\right],\ q = r,t,a \quad (6)$$

Where the shear and edge force coefficients are presented as $K_{qc}(q = r, t, a)$ and $K_{qe}(q = r, t, a)$ respectively. The differential chip width and flute length of the i_{th}cutter element is presented by b_i and S_i respectively. Also, in order to obtain the i_{th} cutter element of the j_{th} flute which is engaged in the cutting process, the $g(\theta_{ij})$ window function is determinate as,

$$g(\theta_{ij}) = \begin{cases} 1, & \theta_{en,ij} \le \theta_{ij} \le \theta_{ex,ij} \\ 0, & Otherwise \end{cases} \quad (7)$$

As a result, the calculated cutting forces in the radial, tangential and axial directions for each cutting element can be transformed into the feed or workpiece coordinate system as,

$$F_{ij}(\theta_{ij}, u) = \begin{bmatrix} F_{x,ij}(\theta_{ij}, u) \\ F_{y,ij}(\theta_{ij}, u) \\ F_{z,ij}(\theta_{ij}, u) \end{bmatrix} = WH_{ij} \begin{bmatrix} F_{r,ij}(\theta_{ij}, u) \\ F_{t,ij}(\theta_{ij}, u) \\ F_{a,ij}(\theta_{ij}, u) \end{bmatrix}, \quad (8)$$

Where,

$$H_{ij} = \begin{bmatrix} -\sin(\theta_{ij}) & -\cos(\theta_{ij}) & 0 \\ -\cos(\theta_{ij}) & \sin(\theta_{ij}) & 0 \\ 0 & 0 & -1 \end{bmatrix} \quad (9)$$

And

$$W = \begin{cases} \begin{bmatrix} 1 & 0 & 0 \\ 0 & 1 & 0 \\ 0 & 0 & 1 \end{bmatrix}, & for\ the\ feed\ cordicate\ frame \\ [x_f \quad y_f \quad z_f], & for\ the\ worjpiece\ cordicate\ frame \end{cases} \quad (10)$$

4. Cutting temperature model

The process of chip formation in the machining operations generates heat in the cutting zone which increases the temperature of cutting tool and workpiece.

The equation of the cutting temperature regarding the cutting parameters is presented by Shaw [24] as,

$$\theta = C_\theta V^{b1} f_z^{b2} a_e^{b3} a_p^{b4} \quad (11)$$

Where θ is temperature of cutting process (degree Celsius), C_θ is temperature coefficient obtained by material of workpiece, machine tool, and cutting tool geometry parameter. The b1, b2, b3, and b4 are exponents influencing the machining parameters V, f_z, a_e and a_p, as cutting speed (m/minutes), feed rate (mm/z), radial feed and axial feed (mm) respectively.

The equations of the cutting tool and workpiece temperatures in the machining operations of AL alloys based on multiple nonlinear regression analysis are presented by Santos et al. [25] as,

$$\theta_t = 116.503\, V^{0.211} f_z^{0.181} a_e^{0.0464} a_p^{0.00391} \quad (12)$$

$$\theta_w = 43.319\, V^{0.365} f_z^{0.244} a_e^{0.0423} a_p^{0.019} \quad (13)$$

Where θ is temperature (degree Celsius), V is cutting speed (m/minutes), $f_z$is feed rate (mm/z), a_e and $a_p$are radial feed and axial feed (mm) respectively.

4- Deflection error analysis of thin-wall workpiece in machining operations

The dimensional error of machined surfaces is the amount of deviation in actual machined surface from the nominal surface of workpiece CAD model. The machining operations of thin walled parts are with deflection error as a result of cutting forces as well as cutting temperature. The workpiece deflects to a new position due to cutting forces and cutting temperatures which creates dimensional error and inaccuracy in process of machining operations. The surface dimensional error due to the cutting forces and cutting temperature is shown in the figure 5 [26].

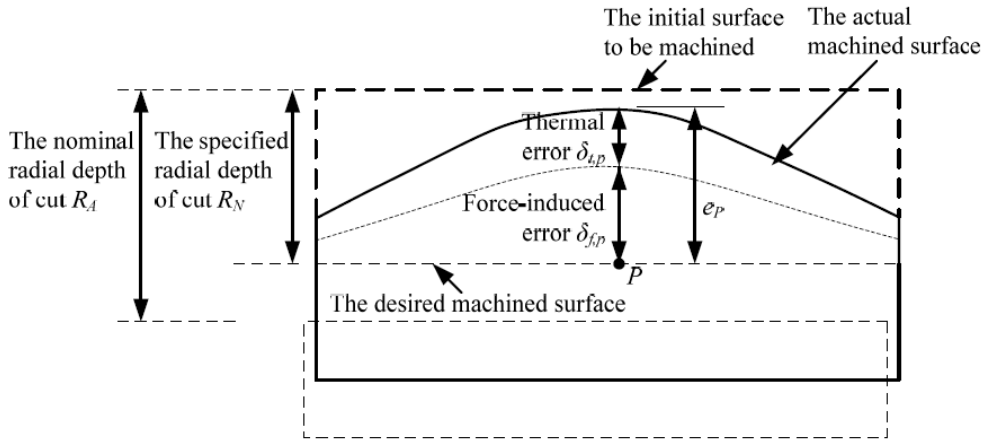

Fig. 5. The surface dimensional error due to the cutting forces and cutting temperature [26].

The corresponding surface dimensional error can be presented as Eq. (14) [26],

$$e_p = \delta_{t,p} + \delta_{f,p} + R_N - R_A \tag{14}$$

Where, $\delta_{t,p}$ and $\delta_{f,p}$ are the normal projections of the cutting force and cutting temperature induced deflection error for the Point P, respectively. Also, R_N and R_A are the nominal and specified radial depth of cut, respectively.

5- Virtual machining system to predict and minimize the deflection error

In order to develop applications of the virtual machining systems in the deflection error prediction and minimization of thin walled machined parts, the Visual Basic programming language is used in the study. Nominal machining path, the geometry and material properties of cutting tool as well as the CAD model of workpiece are input to the system. The developed virtual machining system can obtain the cutting forces regarding the cutting tool details and parameters of machining operations. So, cutting forces at each position of cutting tool along machining paths can be calculated. The cutting force calculator dialogue box is shown in figure 6.

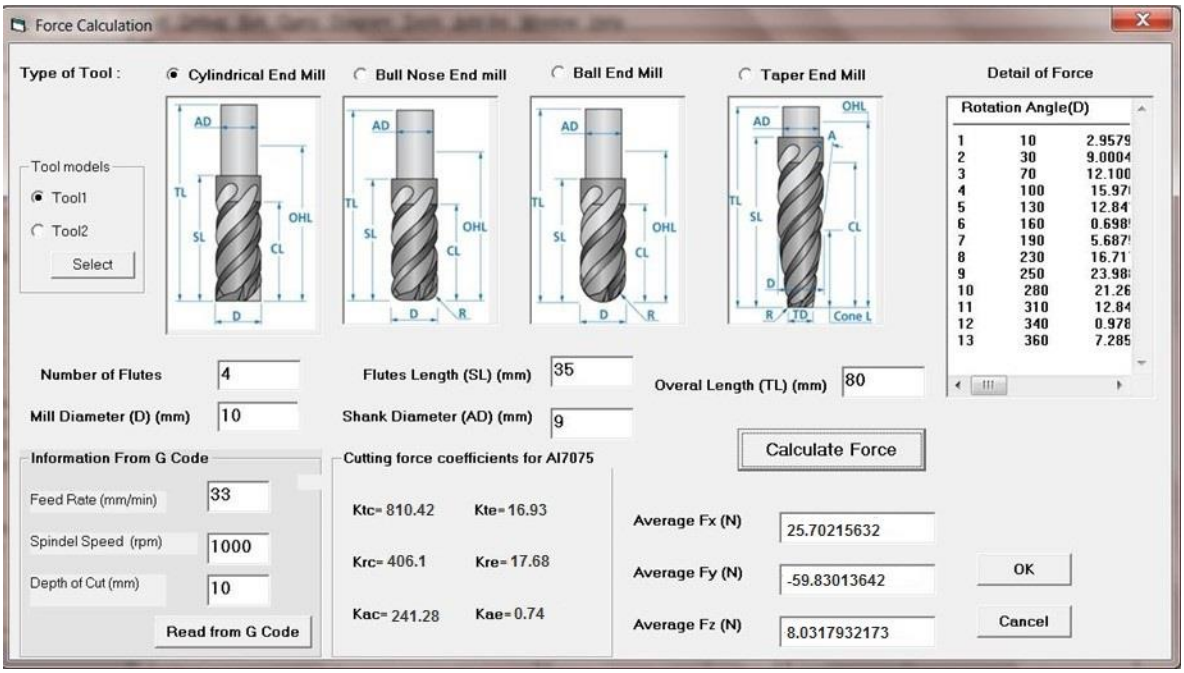

Fig. 6. Dialogue box of cutting force calculator.

In order to obtain the deflection error in the machining operation, the cutting temperature at each position of cutting tool along machining paths is calculated by the developed software. Then, obtained data from the cutting forces as well as cutting temperature are transferred to the Abaqus R2016X FEM analysis software [27] to calculate the deformation error of machined part. The mesh is applied to the CAD model of thin walled impeller blades in order to calculate the temperature and cutting force-induced deflection error in milling operations. The predicted cutting forces and cutting temperature at the each position of cutting tool along machining paths are applied to each node of the meshed model of the workpiece in order to measure node displacement. As a result, the deflection error due to cutting forces and cutting temperatures at each position of cutting tool can be calculated and presented. Flowchart and strategy of the virtual machining system in cutting force calculation and deflection error prediction is shown in the figure 7.

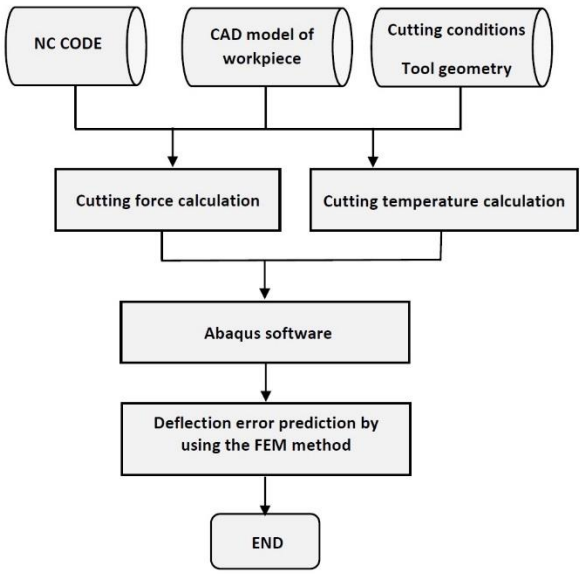

Fig. 7. Flowchart of the virtual machining system in calculation of cutting force, cutting temperature and deflection error prediction.

The appendix A is the developed algorithm of the virtual machining system in the study.
To obtain the optimized machining parameters in terms of deflection error minimizations, the genetic algorithm is applied. The natural process of evolution and set of chromosomes is introduced in terms of optimization process. The initial population for the optimization process is created using the binary encoding process. To provide evaluation criteria in the optimization process and rank the chromosomes in population, the fitness function is calculated as is presented in the Eq. (15) [28].

$$F(x) = \frac{1}{1+f(x)} \tag{15}$$

Where $F(x)$ and $f(x)$ are fitness function and objective function respectively. The reproduction, crossover and mutation are main operators of the algorithms. In order to create a faster convergence to the optimized parameters, The operators as reproduction, crossover and mutation are applied to the initial population of the optimization process. To simulate the surface roughness of machined parts by using the mathematical concepts, the Eq. (16) [29] is presented.

$$R_a = 318\frac{f^2}{4d} \tag{16}$$

Where f is feed rate and d is diameter of cutting tool. Moreover, the time of machining operation should be minimized in order to decrease cost of machined parts. The mathematical equation of machining time is presented in the Eq. (17) [29].

$$t_m = \frac{k}{f} \tag{17}$$

Where k is the distance of cutting tool to reach to the operational zone and f is feed rate.

Also, cutting tool life should be maximized in the optimization process in order to decrease the cost of machining operation. The cutting tool life can be shown as the Eq. (18) [29].

$$T_L = \left(\frac{60}{Q}\right)\left[\frac{C\left(\frac{G}{5}\right)}{V(A)^w}\right]^{\frac{1}{m}} \tag{18}$$

Where Q is the contact proportion of cutting edge with workpiece per revolution, C is 33.98 for the HSS tools and 100.05 for the carbide tools, $g = 0.14$, V is cutting speed (mm/minutes) , $w = 0.28$, m is 0.15 for HSS tools while it reaches a maximum of 0.30 for carbide tools, $G$and A are slenderness ratio and chip cross-section which can be shown as Eq. (19) and Eq. (20) respectively [29].

$$G = \frac{a}{f} \tag{19}$$

$$A = a.f \tag{20}$$

Where a depth of cut and f is feed rate in machining operations.
According to the Eq. (12) and Eq. (13), the cutting temperature can be reduced by decreasing the feed rate and spindle speed. Also, according to the Eq. (16), the surface roughness can be decreased by reducing the feed rate. But, the machining time will be increased by reducing the feed rate according to the Eq. (17). Moreover, increasing the spindle speed can decrease the cutting forces according to the Eq. (8) and cutting tool life according to the Eq. (18). It is clear that the presented mathematical models of the cutting forces, cutting temperature, time of machining operations, surface roughness, feed rate and cutting tool life are related together which should be considered as an optimization problem. As a result, an optimization process of machining parameters as is shown in the figure 8 should be implemented to calculate the optimized feed rate and spindle speed in machining operations.

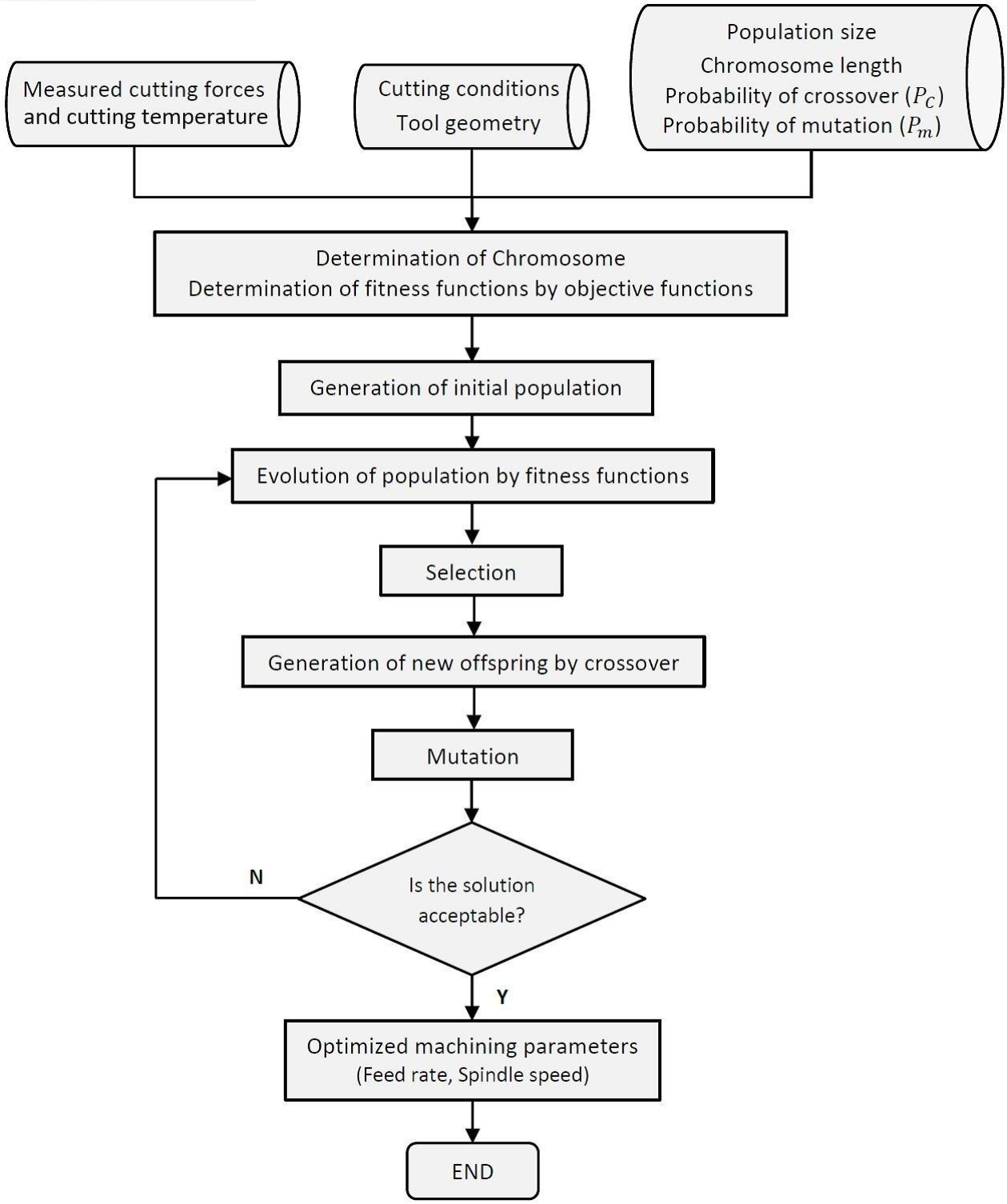

Fig. 8. The optimization process of machining parameters.

In the appendix B, the optimization method algorithm is described.
The Matlab programming language is used to obtain the optimized machining parameters in order to minimize the deflection error. As a result, optimized feed rate and spindle speed are obtained in order to minimize the deflection errors in milling operations of thin walled impellers.

7. Validation

The impeller is machined by using the A 5-axis CNC milling machine tool Kondia HM 1060 In order to validate the presented virtual machining system in the study. The impeller material is AL 7075. The dimensions of Al impeller in millimeter unit is shown in the Figures 9.

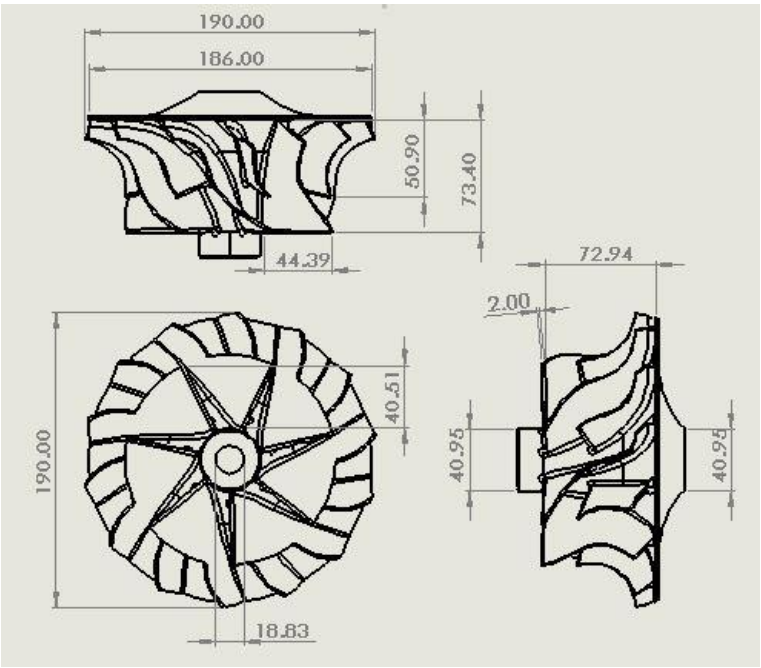

Fig. 9. Dimensions of AL blade in millimeter unit.

Mechanical properties of AL 7075 is presented in table 1.

Property	Value	Units
Elastic Modulus	7.17 e^+10	N/m^2
Poisson's Ratio	0.33	N/A
Shear Modulus	1.6e+8	N/m^2
Mass Density	2810	kg/m^3
Tensile Strength	5.3e+8	N/m^2
Ultimate Tensile Strength	5.72e+8	N/m^2
Yield Strength	5e+8	N/m^2
Thermal Expansion	2.2 e^-05	/k
Thermal Conductivity	196	w/(m.k)
Specific Heat	714.8	J/(kg.k)

Table. 1. Mechanical properties of AL 7075.

To simulate machining operations of impeller by using a 5-Axis CNC milling machine tool, the Masterccam software [30] is used. The cutting tool paths and machining strategies is shown in the figure 10.

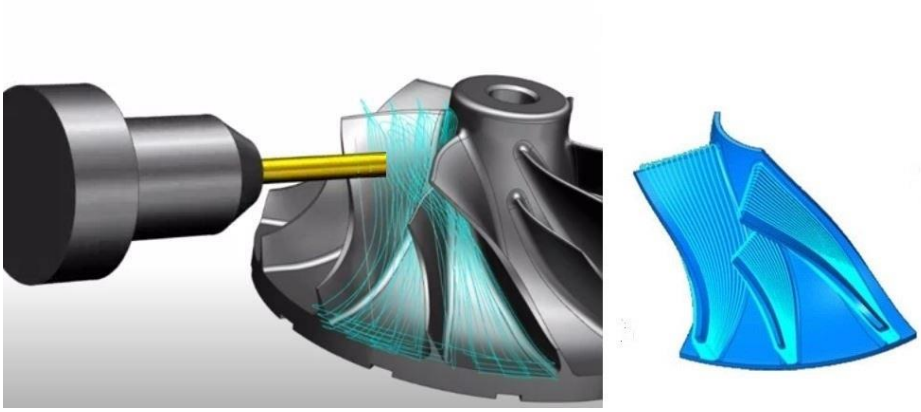

Fig. 10. The machining strategies and cutting tool paths.

Then, the test impellers are machined by using the 5-axis Kondia HM 1060 CNC machine tool. The cutting tool used in the experiment is carbide end mill with 8 mm diameter, helix angel 30°, flute number 4, overall length 60 mm and flute length 35 mm. The spindle speed and feed rate are 200 m/min and 200 mm/min respectively. The machining operation of turbine blade is shown in the figure 11.

Fig. 11. Machining operation of impeller.

The real machined AL impeller is shown in the figure 12.

Fig. 12. The real machined AL impeller.

The deflection error in the machined impeller blade is measured by using the CMM machine. The Renishaw RSH 250 probe [31] is used in order to measure deflection error of machined impeller blade while its repeated accuracy is 1 µm in touching directions. The process of measuring the machined impeller is shown in the figure 13.

Fig. 13. The measuring process of the machined impeller blade.

The procedure measuring the machined impeller blade by using the CMM is shown in the figure 14.

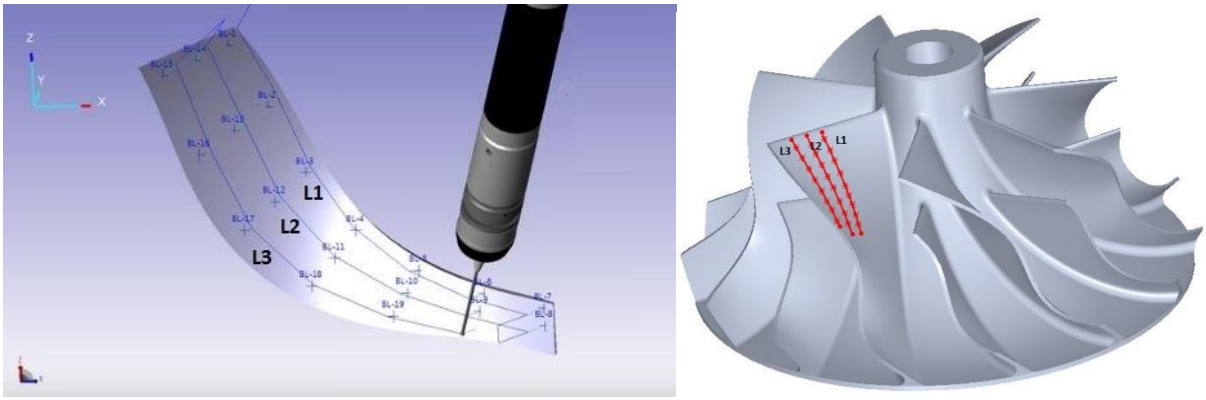

Fig. 14. Procedure of impeller blade measuring by using the CMM.

The cutting force model of 5-axis CNC machine tools in machining operations of thin walled parts presented by Zhang et al. [32] is used in this study to calculate the cutting forces in virtual environments. The average of cutting forces for milling operations of thin walled blades by using 5-axis CNC milling machine tool Kondia HM 1060 are measured by Kistler dynamometer in order to calculate the coefficients of specific cutting force. The spindle rotating speed is 3000 rpm and the feed per tooth and feed rate are 0.5 mm 100 mm/min respectively. As result, the specific cutting force coefficients are obtained as Table 2.

The specific cutting force coefficients	$K_{rc}\ (N/mm^2)$	$K_{re}\ (N/mm)$	$K_{tc}\ (N/mm^2)$	$K_{te}\ (N/mm)$	$K_{ac}\ (N/mm^2)$	$K_{ae}\ (N/mm)$
	406.1	17.68	810.42	16.93	241.28	0.74

Table 2. The specific cutting force coefficients.

The Abaqus software [27] is used to measure the deflection errors of impeller blade due to the cutting forces and cutting temperature. So, the calculated deflection error of the machined thin-walled impeller by using the FEM method is shown in the figure 15.

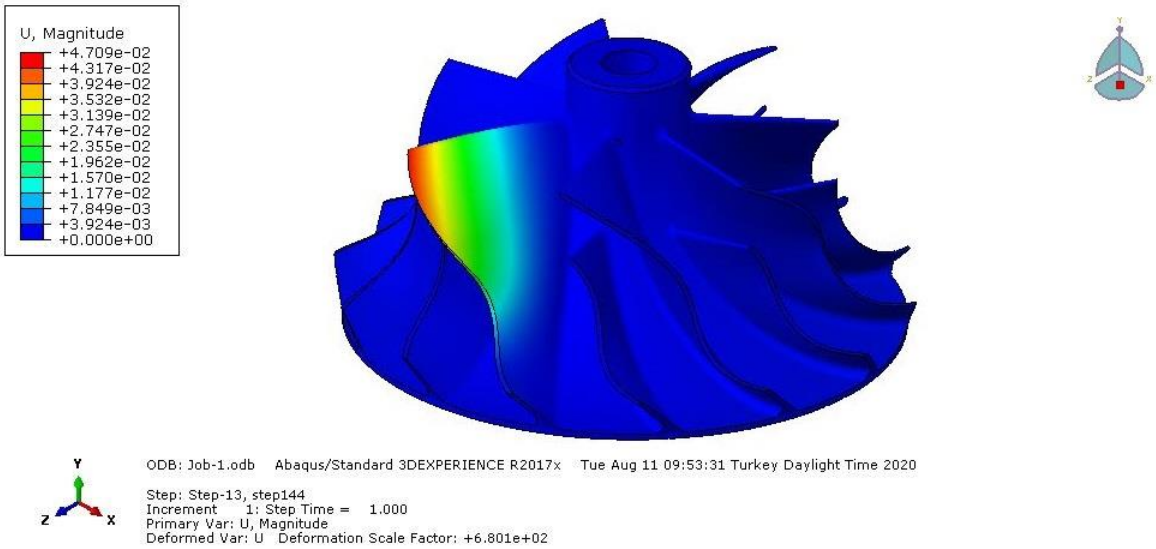

Fig. 15. The calculated deflection error of the machined thin walled impeller by using the FEM.

As a result, the measured and FEM simulated deflection errors in the thin-walled impeller blade are obtained as is shown in the figure 16.

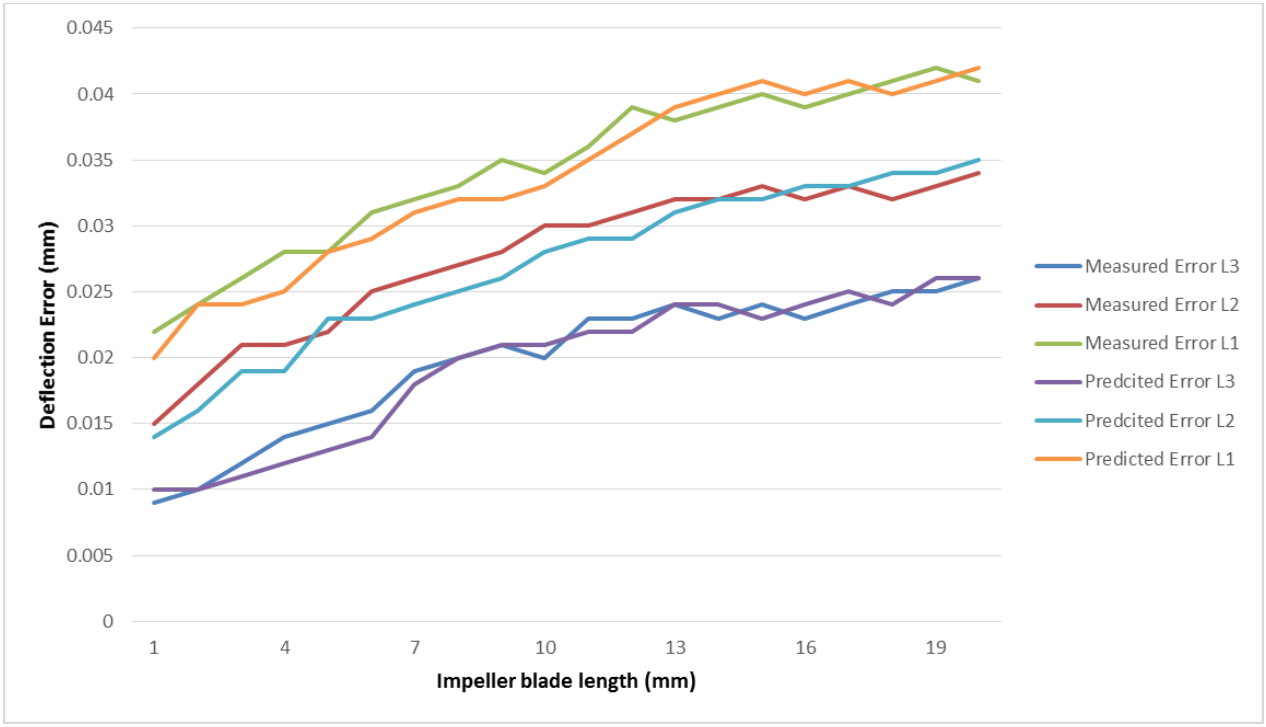

Fig. 16. The measured and predicted deflection errors in the machined thin-walled impeller blade.

A good compatibility is obtained in comparison of the results of the experimental test and predicted deflection error of the machined thin-walled impeller. Optimized machining parameters are calculated using the developed optimization techniques in the study based on the genetic algorithm. To measure the cutting forces in the machining operation, the Kistler dynamometer is used. Then, the measured cutting forces are applied in the optimization algorithm of the figure 8 and appendix B in order to provide input data for the optimization process. In the optimization process, the population size of 39 is selected with the iterated for 306 generations. Also, the probability of crossover of 0.68 and mutation of 0.001 are selected. As a result, the feed rate 170 mm/min and the spindle speed 260 m/min are obtained. Measured and predicted surfaces roughness of machined turbine blade by using optimized machining parameters is shown in the figure 17.

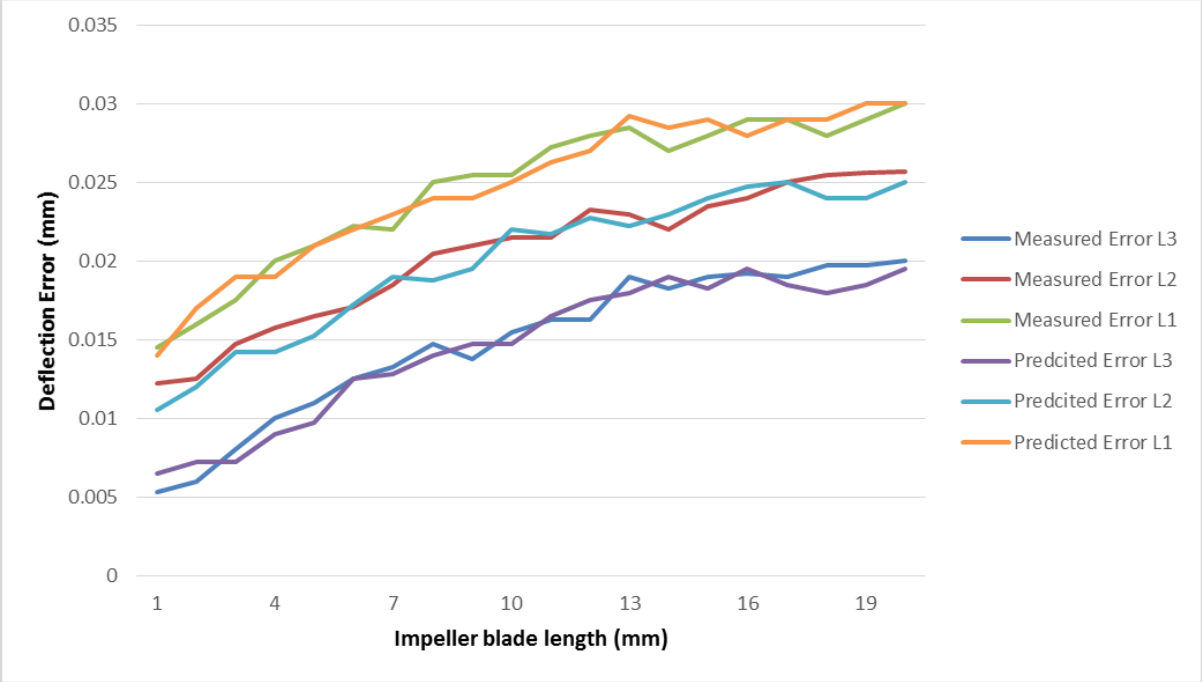

Fig. 17. Measured and predicted deflection error of machined thin-walled impeller blade by using optimized machining parameters.

8. Conclusion

An application of virtual machining system is developed in the study in order to predict and minimize the deflection errors in 5-Axis milling operations of thin walled impellers. So, the cutting forces and cutting temperature at each position of cutting tool along machining paths is calculated by by considering the CAD model of workpiece, cutting conditions and cutting tool geometries. The Finite Element Method is used to obtain the deflection error in the thin wall workpiece. To validate the developed method in the study, a real impeller is machiied by using the 5-Axis CNC machine tool. To obatin the deflection error, the machind blade is measured by using the CMM machine. To calculate the compatibility rate in the developed system, the obtained results from the virtual machining system and experimental tests are compared. A 91.6% compatibility in comparison to the experimental and virtual machining system results is obtained. To minimize the residual stress in machining operation, optimized machining parameters using the Genetic algorithm is obtained. As a result, 24.4% reduction in defelction error of machined impeller blade is obtained using the optimized machining parameters. So, the developed method in the study can decrease the defelction error in the machining operations of the thin walled impeller baldes to increase accuracy and efficiency in

part menaufacturing process. Furthermore, it is concluded that applications of the optimizations techniques in the virtual machining systems can increase accuracy and reliability of machined parts by using machining oerations. The method can be applied to the more soghistacted parts with free form surfaces such as turbine baldes in order to increase accuracy of machined thin walled surfaces due to deflection error redcution. To enhance the qulaity of machined parts, the deflection errors in the cutting tool and workpiece due to cutting forces can be predcited and compenstaed. Morover, the developed system in the study can be applied to the surfaces quality of macined parts in order to be improved. These are future reaserch works of the authours.

9. Declarations

Availability of data and materials

All data and materilas of the research work were availabile for the authors.

Acknowledgements

Not applicable.

Authors' contributions

Mohsen Soori conceived the idea and completed most of the research work, then wrote the manuscript. Mohammed Asmael guided the reseach plan and gave advices on the research work and manuscript. All authors read and approved the final manuscript.

Funding

Supported by Department of Mechanical Engineering, Eastern Mediterranean University, Famagusta, North Cyprus, Via Mersin 10, Turkey.

Competing interests

The authors declare no competing financial interests.

References

1. Artetxe E, González H, Calleja A, Valdivielso AF, Polvorosa R, Lamikiz A, Lacalle LNLD (2016) Optimised methodology for aircraft engine IBRs five-axis machining process. International Journal of Mechatronics and Manufacturing Systems 9 (4):385-401
2. Zhao Z, Wang Y, Qian N, Su H, Fu Y (2020) A framework for accuracy enhancement in milling thin-walled narrow-vane turbine impeller of NiAl-based superalloy. The International Journal of Advanced Manufacturing Technology:1-14
3. Huang T, Zhang X-M, Ding H (2017) Tool orientation optimization for reduction of vibration and deformation in ball-end milling of thin-walled impeller blades. Procedia CIRP 58:210-215
4. Chaves-Jacob J, Poulachon G, Duc E (2012) Optimal strategy for finishing impeller blades using 5-axis machining. The International Journal of Advanced Manufacturing Technology 58 (5-8):573-583
5. Huang N, Bi Q, Wang Y, Sun C (2014) 5-Axis adaptive flank milling of flexible thin-walled parts based on the on-machine measurement. International Journal of Machine Tools and Manufacture 84:1-8

6. Liu ZG, Qi HJ, Cai YJ Research on the Method of Error Prediction in Milling Thin-Walled Impeller Blade. In: Materials Science Forum, 2012. Trans Tech Publ, pp 124-129
7. Khandagale P, Bhakar G, Kartik V, Joshi SS (2018) Modelling time-domain vibratory deflection response of thin-walled cantilever workpieces during flank milling. Journal of Manufacturing Processes 33:278-290
8. Kang Y-G, Wang Z-Q (2013) Two efficient iterative algorithms for error prediction in peripheral milling of thin-walled workpieces considering the in-cutting chip. International Journal of Machine Tools and Manufacture 73:55-61
9. Del Sol I, Rivero A, López de Lacalle LN, Gamez AJ (2019) Thin-Wall Machining of Light Alloys: A Review of Models and Industrial Approaches. Materials 12 (12):2012
10. Bolar G, Joshi SN (2020) Investigations into the influence of tool helix angle during end milling of open straight and curved thin-wall parts. International Journal of Machining and Machinability of Materials 22 (3-4):212-232
11. de Oliveira EL, de Souza AF, Diniz AE (2018) Evaluating the influences of the cutting parameters on the surface roughness and form errors in 4-axis milling of thin-walled free-form parts of AISI H13 steel. Journal of the Brazilian Society of Mechanical Sciences and Engineering 40 (7):334
12. Bolar G, Joshi SN (2018) Numerical Modeling and Experimental Validation of Machining of Low-Rigidity Thin-Wall Parts. In: Precision Product-Process Design and Optimization. Springer, pp 99-122
13. Li Z-L, Zhu L-M (2019) Compensation of deformation errors in five-axis flank milling of thin-walled parts via tool path optimization. Precision Engineering 55:77-87
14. Gang W, Li W-l, Fan R, He Z-r, Yin Z-p (2019) Multi-parameter optimization of machining impeller surface based on the on-machine measuring technique. Chinese Journal of Aeronautics 32 (8):2000-2008
15. Ratchev S, Liu S, Becker A (2005) Error compensation strategy in milling flexible thin-wall parts. Journal of Materials Processing Technology 162:673-681
16. Dimopoulos CA, Gantes CJ (2012) Experimental investigation of buckling of wind turbine tower cylindrical shells with opening and stiffening under bending. Thin-Walled Structures 54:140-155
17. Buckney N, Pirrera A, Green SD, Weaver PM (2013) Structural efficiency of a wind turbine blade. Thin-Walled Structures 67:144-154
18. Soori M, Arezoo B, Habibi M (2017) Accuracy analysis of tool deflection error modelling in prediction of milled surfaces by a virtual machining system. International Journal of Computer Applications in Technology 55 (4):308-321
19. Soori M, Arezoo B, Habibi M (2014) Virtual machining considering dimensional, geometrical and tool deflection errors in three-axis CNC milling machines. Journal of Manufacturing Systems 33 (4):498-507
20. Soori M, Arezoo B, Habibi M (2013) Dimensional and geometrical errors of three-axis CNC milling machines in a virtual machining system. Computer-Aided Design 45 (11):1306-1313
21. Soori M, Arezoo B, Habibi M (2016) Tool deflection error of three-axis computer numerical control milling machines, monitoring and minimizing by a virtual machining system. Journal of Manufacturing Science and Engineering 138 (8)
22. Altintas Y, Merdol S (2007) Virtual high performance milling. CIRP annals 56 (1):81-84
23. Li Z-L, Tuysuz O, Zhu L-M, Altintas Y (2018) Surface form error prediction in five-axis flank milling of thin-walled parts. International Journal of Machine Tools and Manufacture 128:21-32
24. Shaw MC (2005) METAL CUTTING PRINCIPLES.
25. Santos MC, Machado AR, Barrozo MA (2018) Temperature in Machining of Aluminum Alloys. In: Temperature Sensing. IntechOpen,
26. Huang Y, Zhang X, Xiong Y (2012) Finite element analysis of machining thin-wall parts: error prediction and stability analysis. Finite Element Analysis—Applications in Mechanical Engineering 392
27. About Abaqus software. https://www.3ds.com/products-services/simulia/products/abaqus/. Accessed 06 May 2020

28. Palanisamy P, Rajendran I, Shanmugasundaram S (2007) Optimization of machining parameters using genetic algorithm and experimental validation for end-milling operations. The International Journal of Advanced Manufacturing Technology 32 (7-8):644-655
29. Tolouei-Rad M, Bidhendi I (1997) On the optimization of machining parameters for milling operations. International Journal of Machine Tools and Manufacture 37 (1):1-16
30. About Mastercam software. https://www.mastercam.com/. Accessed 06 May 2020
31. About the Renishaw RSH 250 Probe. https://www.renishaw.com/cmmsupport/knowledgebase/en/rsp2--22120. Accessed August 11 2020
32. Zhang X, Zhang J, Pang B, Zhao W (2016) An accurate prediction method of cutting forces in 5-axis flank milling of sculptured surface. International Journal of Machine Tools and Manufacture 104:26-36

Appendix A

1- Input
Read G-Codes to obtain (G01, G02, G03, X, Y, Z, R, Feed rate, Depth of cut and Spindle Speed)
2- Calculation of cutting forces
Enter the specifications and details of cutting tool as (Flat end, Ball nose end, Ball end, Taper end) and (Lengths, Number of flutes, Diameters)
Obtain the cutting forces along machining paths using the cutting force coefficient (Kts, Krs, Kas, Ktp, Krp, Kap)
Transfer the calculated amount of the cutting forces to the Abaqus software to obtain the residual stress
3- Calculation of cutting temperature
Obtain the temperature of cutting tool and workpiece along machining paths
Transfer the calculated amount of the cutting temperature to the Abaqus software to obtain the residual stress
4- Minimizing the deflection error
Calculate the optimized parameters of machining operation using the Appendix B
Calculate the cutting forces and cutting temperature by using optimized machining parameters for each position of cutting tool along machining paths
Transfer the optimized amount of the cutting forces to the Abaqus software to calculate minimum of the deflection error
5- Output
Generate new G-Codes with optimized machining parameters

Appendix B

1 Generate the binary codes from the parameters of machining operation
2 Calculate the fitness function of the optimization process
3 Create the initial population from the produced binary codes
4 Asses the initial population using the fitness functions
5 Implement the crossover to generate new chromosomes in the initial population
6 Apply mutation
7 Asses the initial population using constrains
8 Check the result regarding the acceptable condition
9 If the result is OK
10 Go to the 14
11 Else

13 Go to the 4
14 End if
15 Print the optimized parameters of machining operation
16 END

Figures

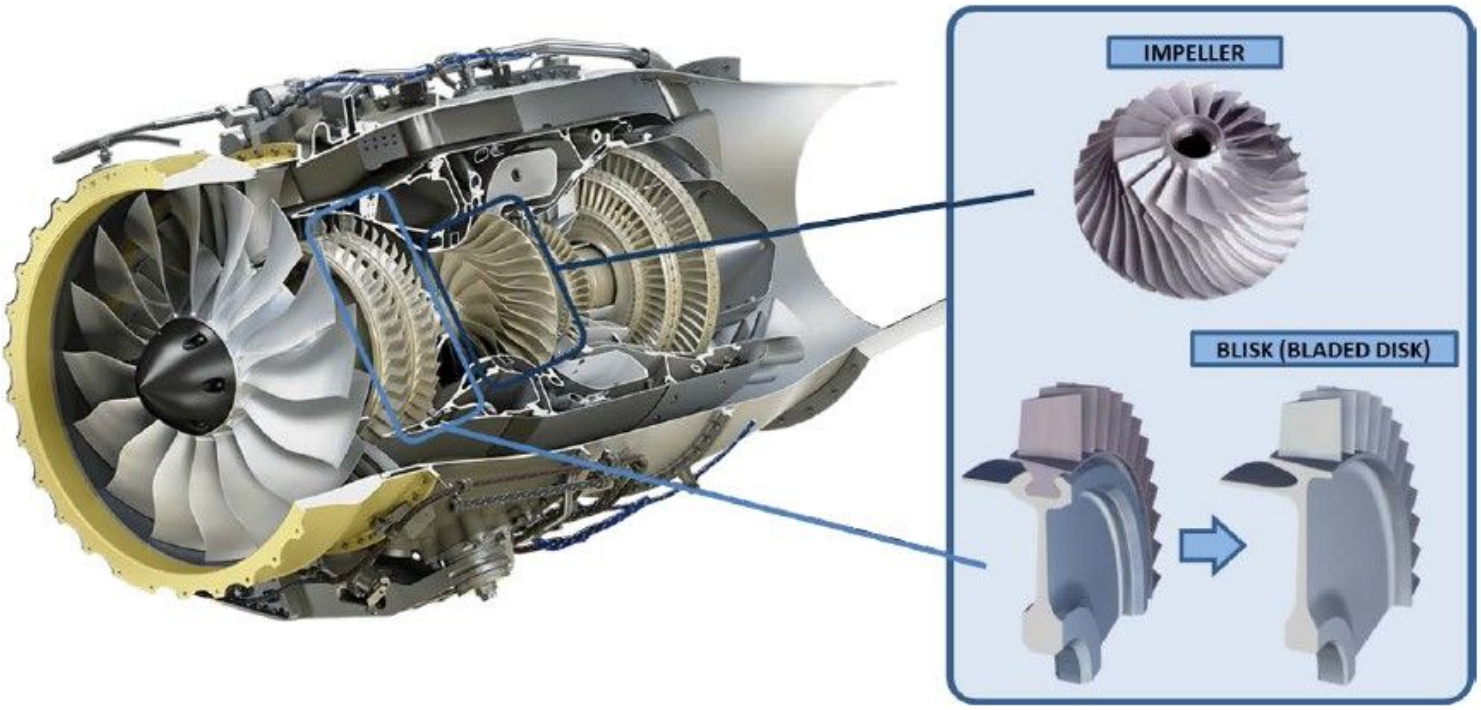

Figure 1

Application of Blisk and impeller in the HF-120 turbofan engine (GE-Honda) [1].

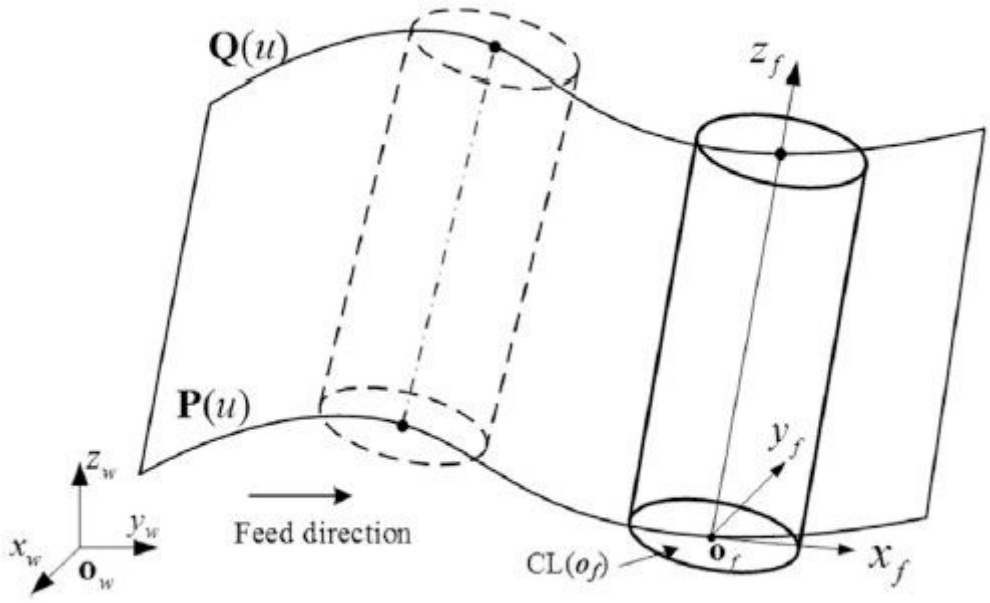

Figure 2

General spatial motion of the end-mill in 5-Axis milling operation [23].

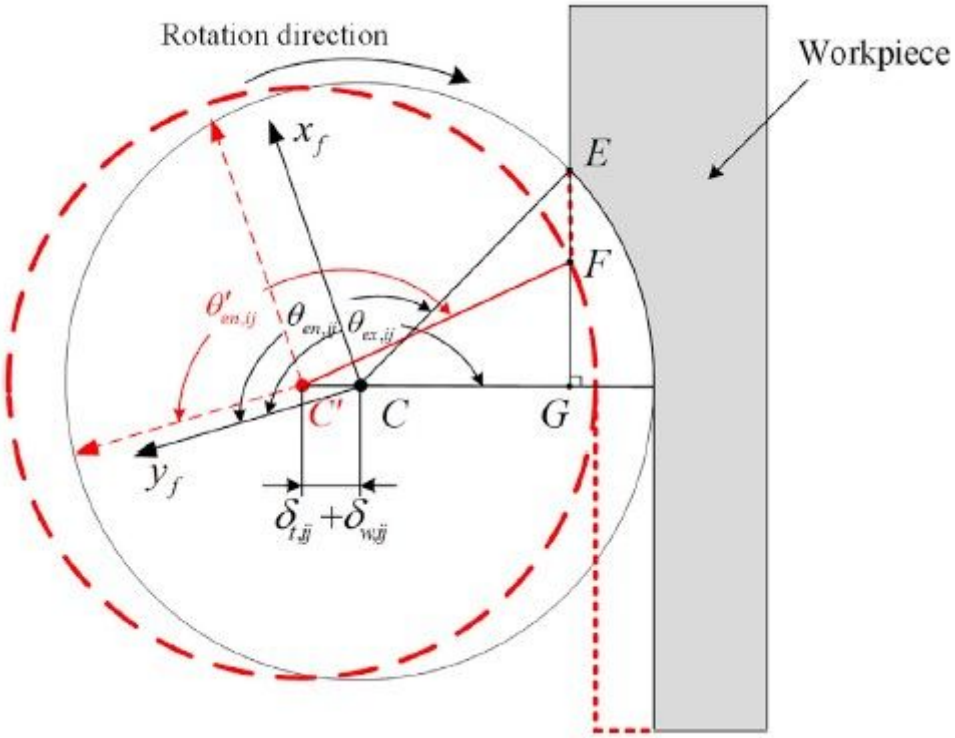

Figure 3

The entry angle for the i_th cutting element of cutting tool during the five axis milling of thin walled workpiece [23].

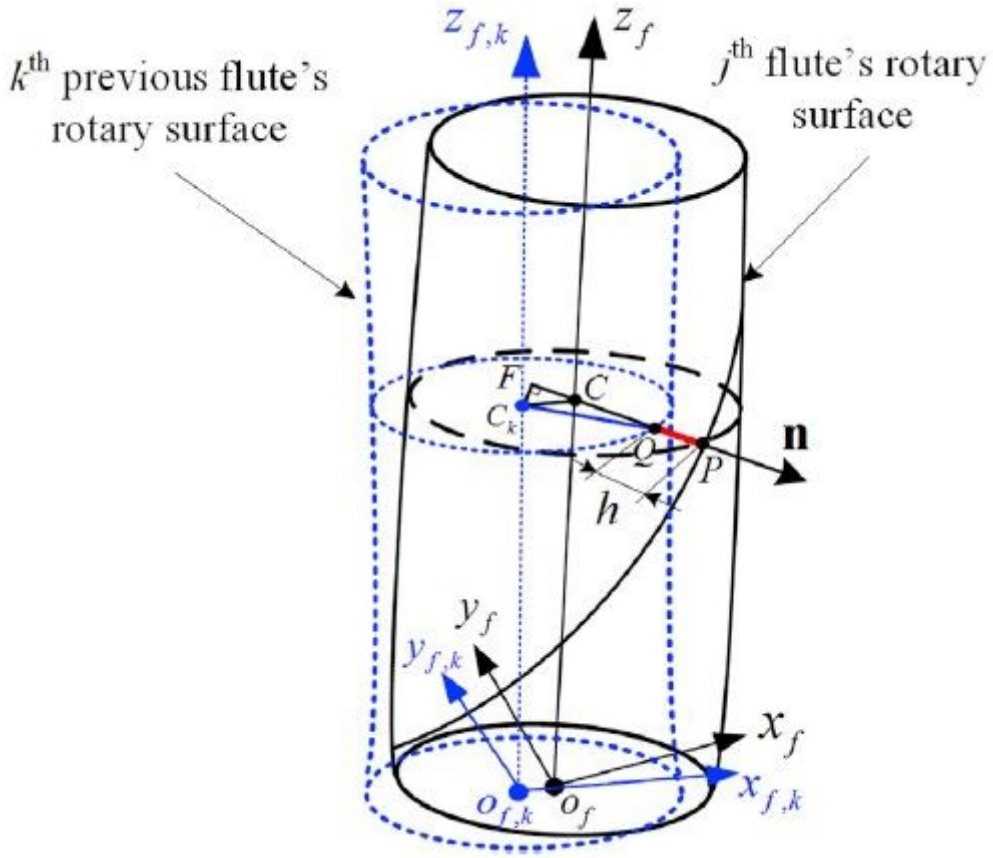

Figure 4

The instantaneous uncut chip thickness calculation by considering the cutter runout during the five axis milling operations of thin walled parts [23].

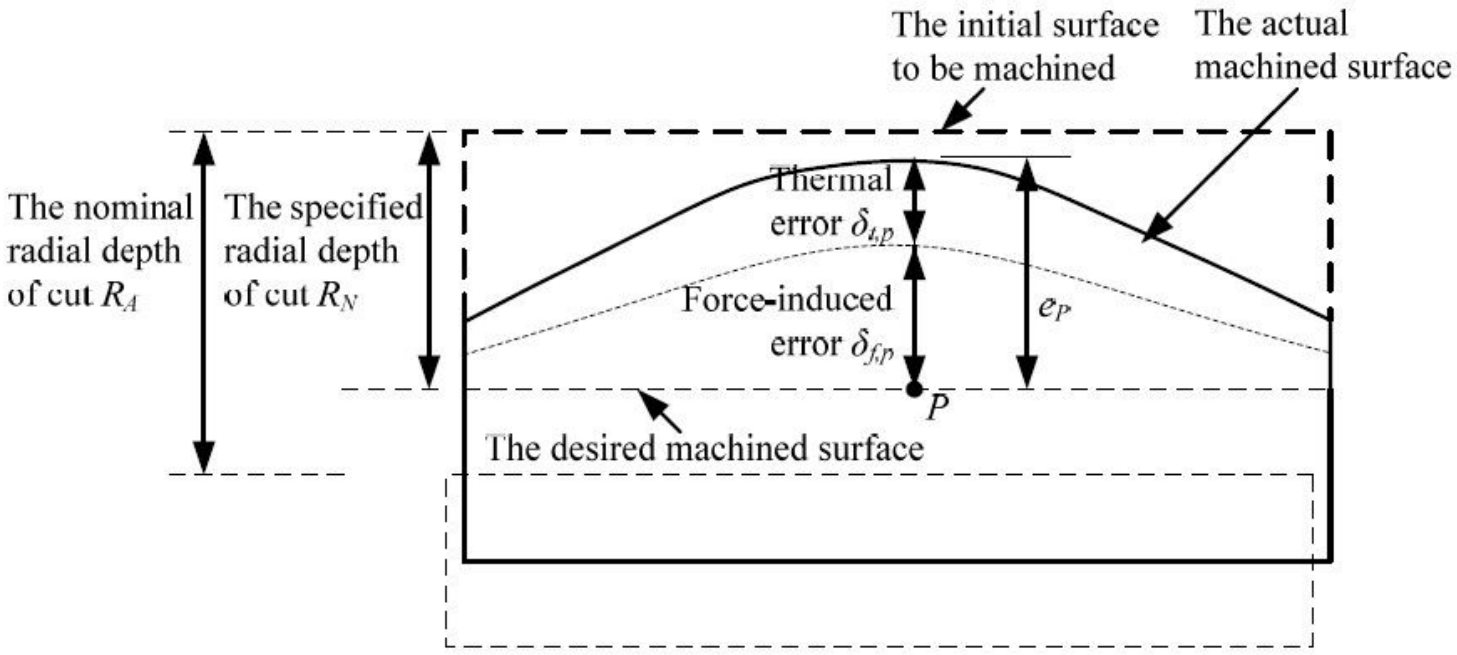

Figure 5

The surface dimensional error due to the cutting forces and cutting temperature [26].

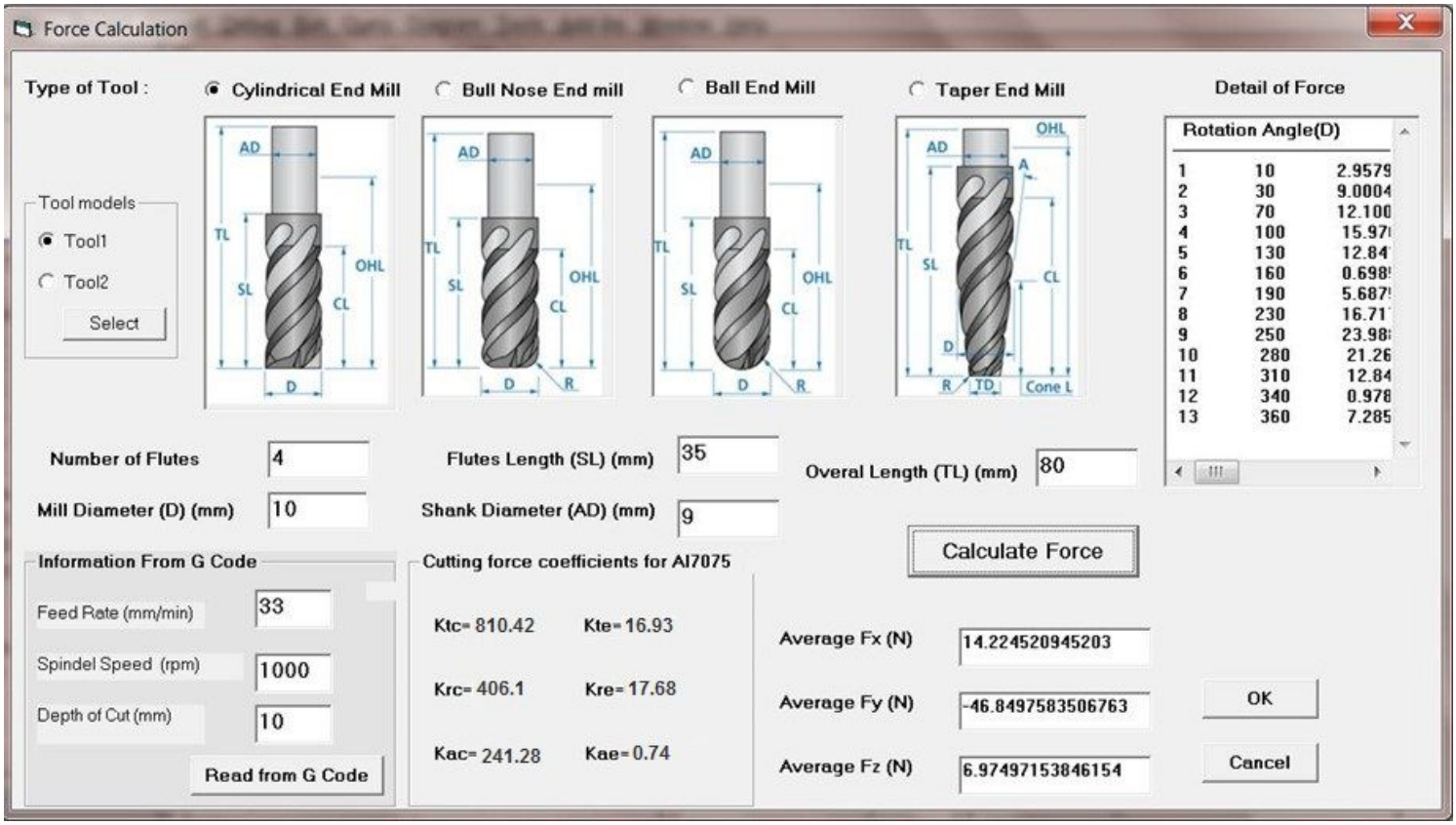

Figure 6

Dialogue box of cutting force calculator.

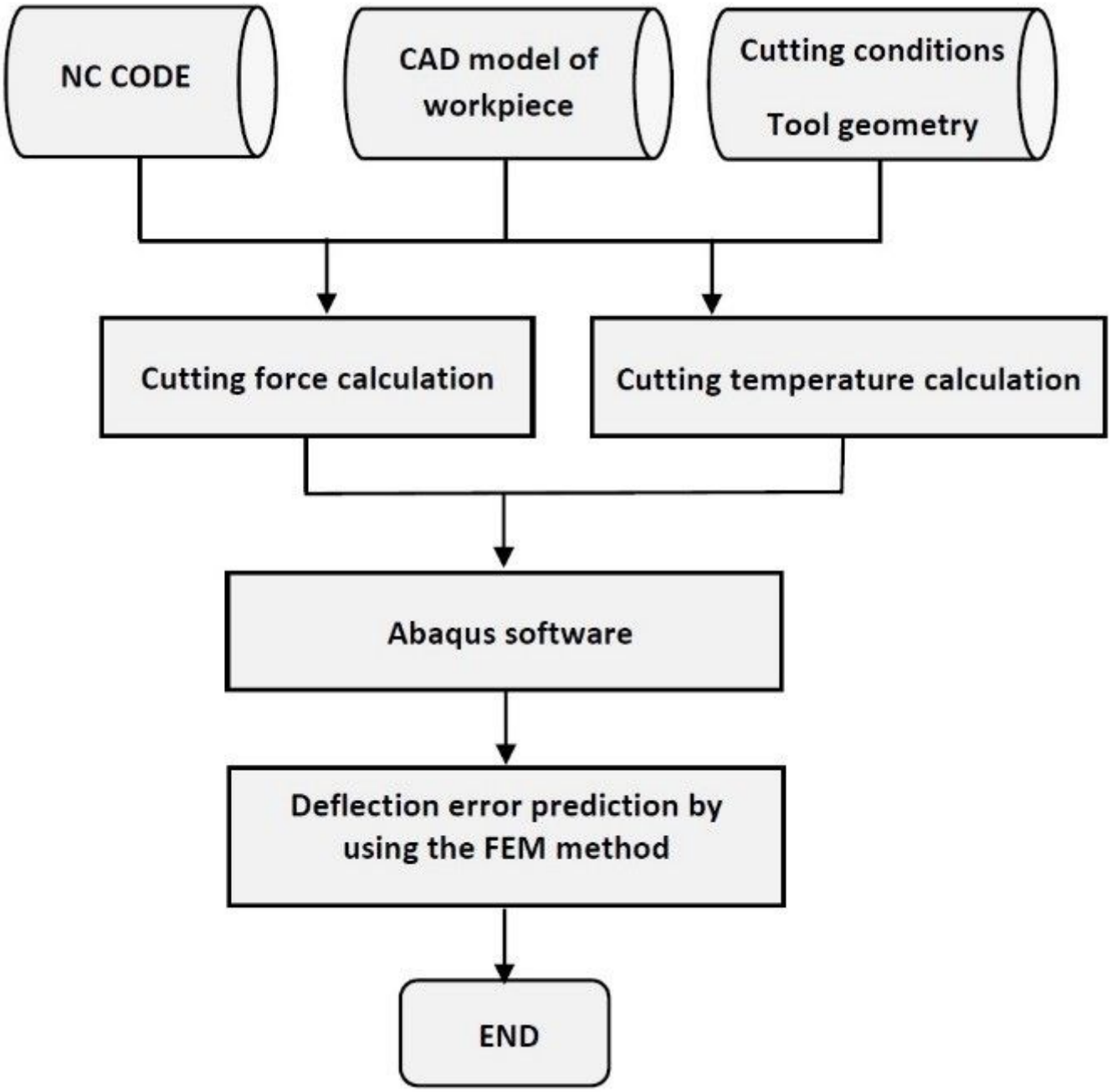

Figure 7

Flowchart of the virtual machining system in calculation of cutting force, cutting temperature and deflection error prediction.

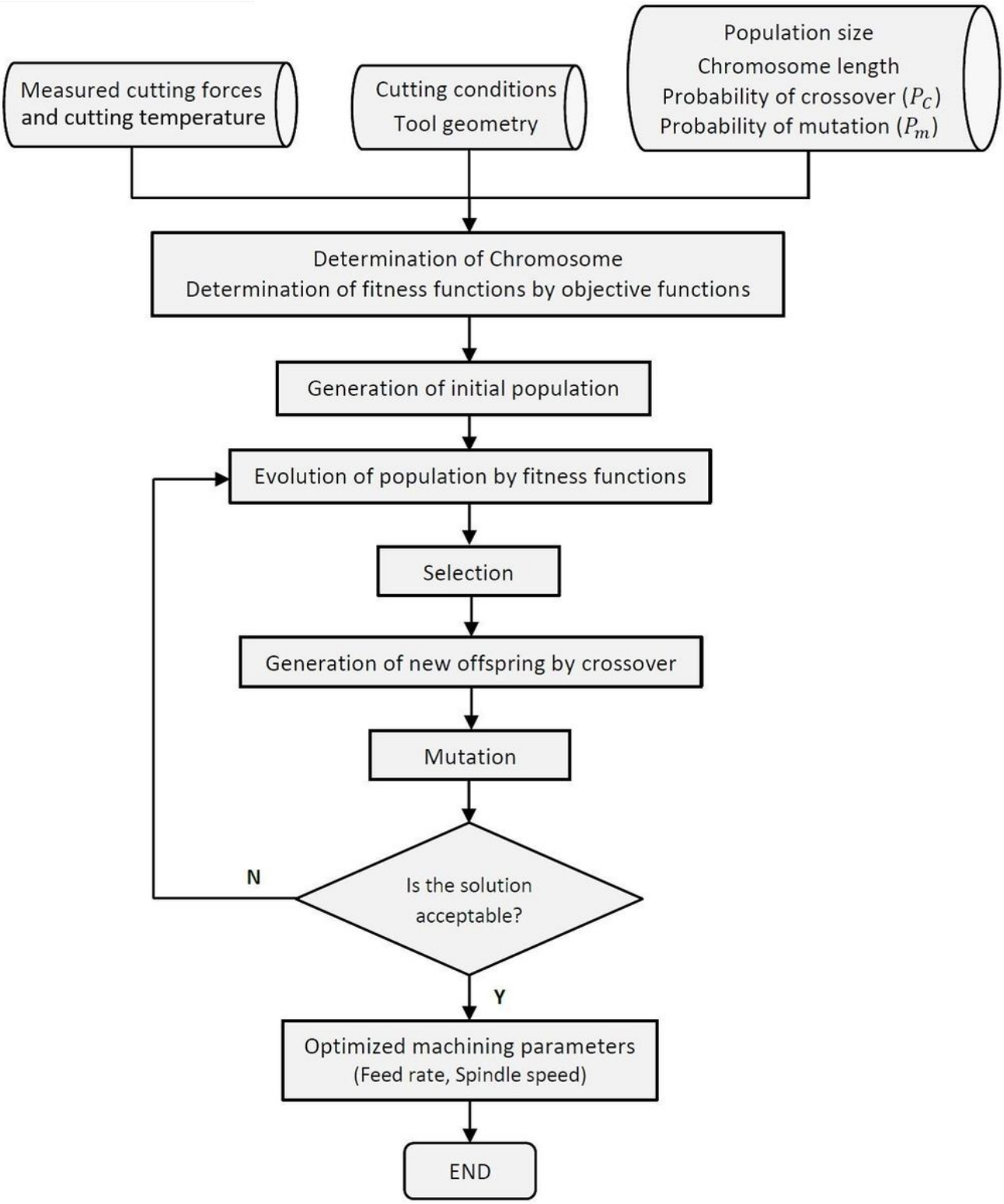

Figure 8

The optimization process of machining parameters.

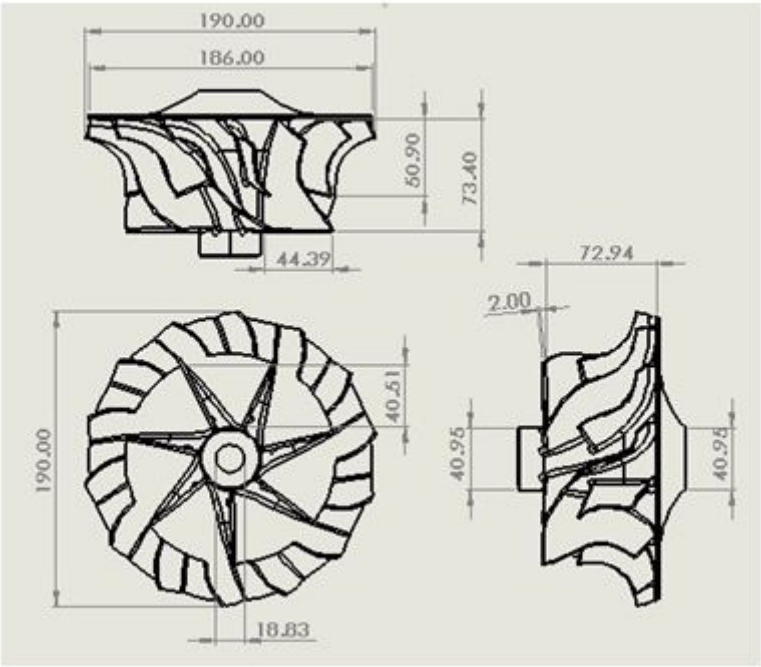

Figure 9

Dimensions of AL blade in millimeter unit.

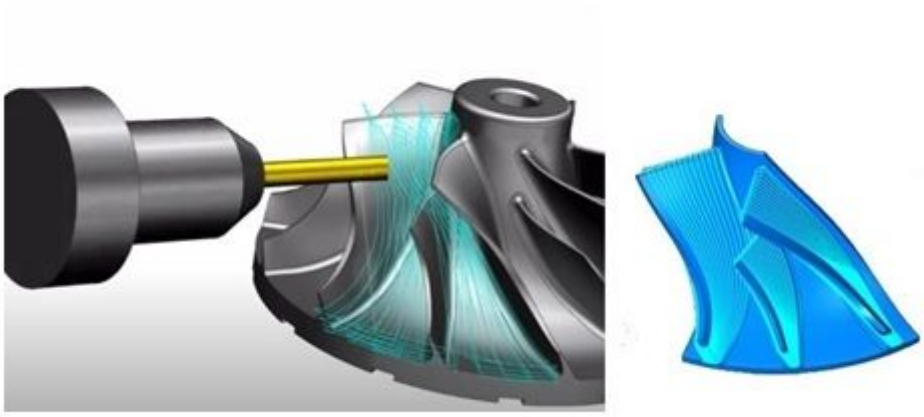

Figure 10

The machining strategies and cutting tool paths.

Figure 11

Machining operation of impeller.

Figure 12

The real machined AL impeller.

Figure 13

The measuring process of the machined impeller blade.

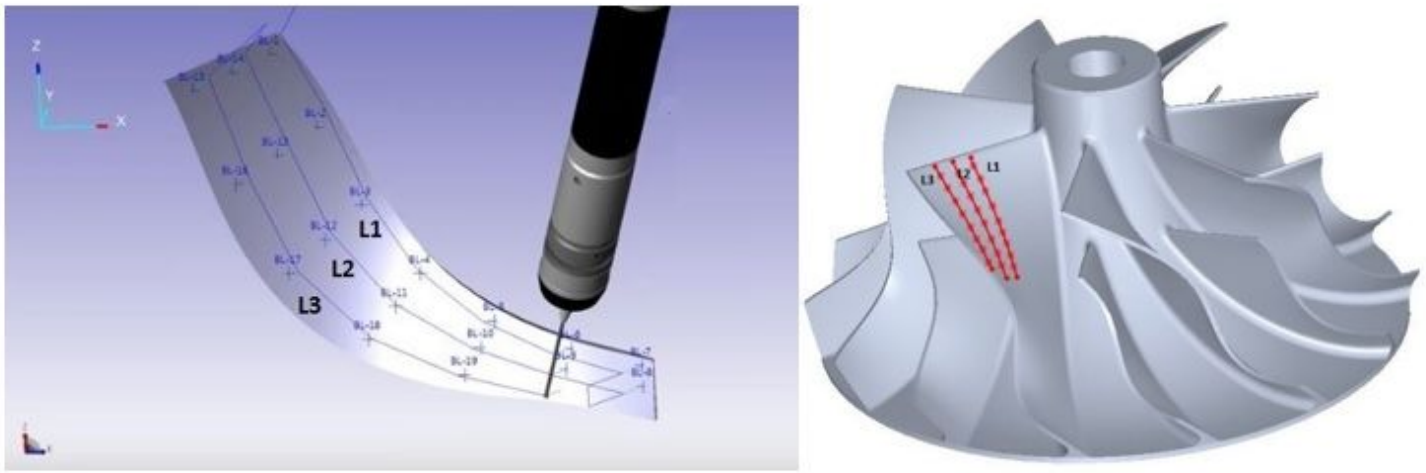

Figure 14

Procedure of impeller blade measuring by using the CMM.

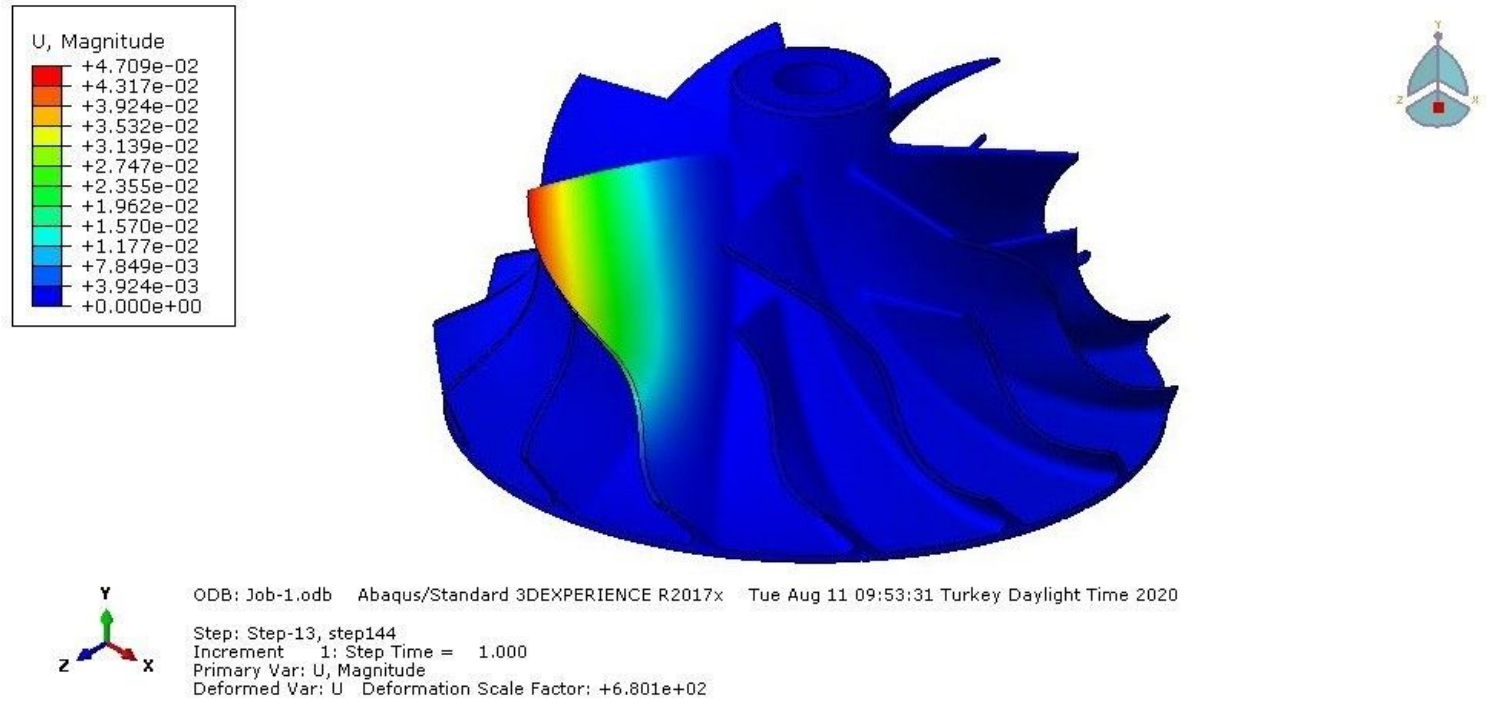

Figure 15

The calculated deflection error of the machined thin walled impeller by using the FEM.

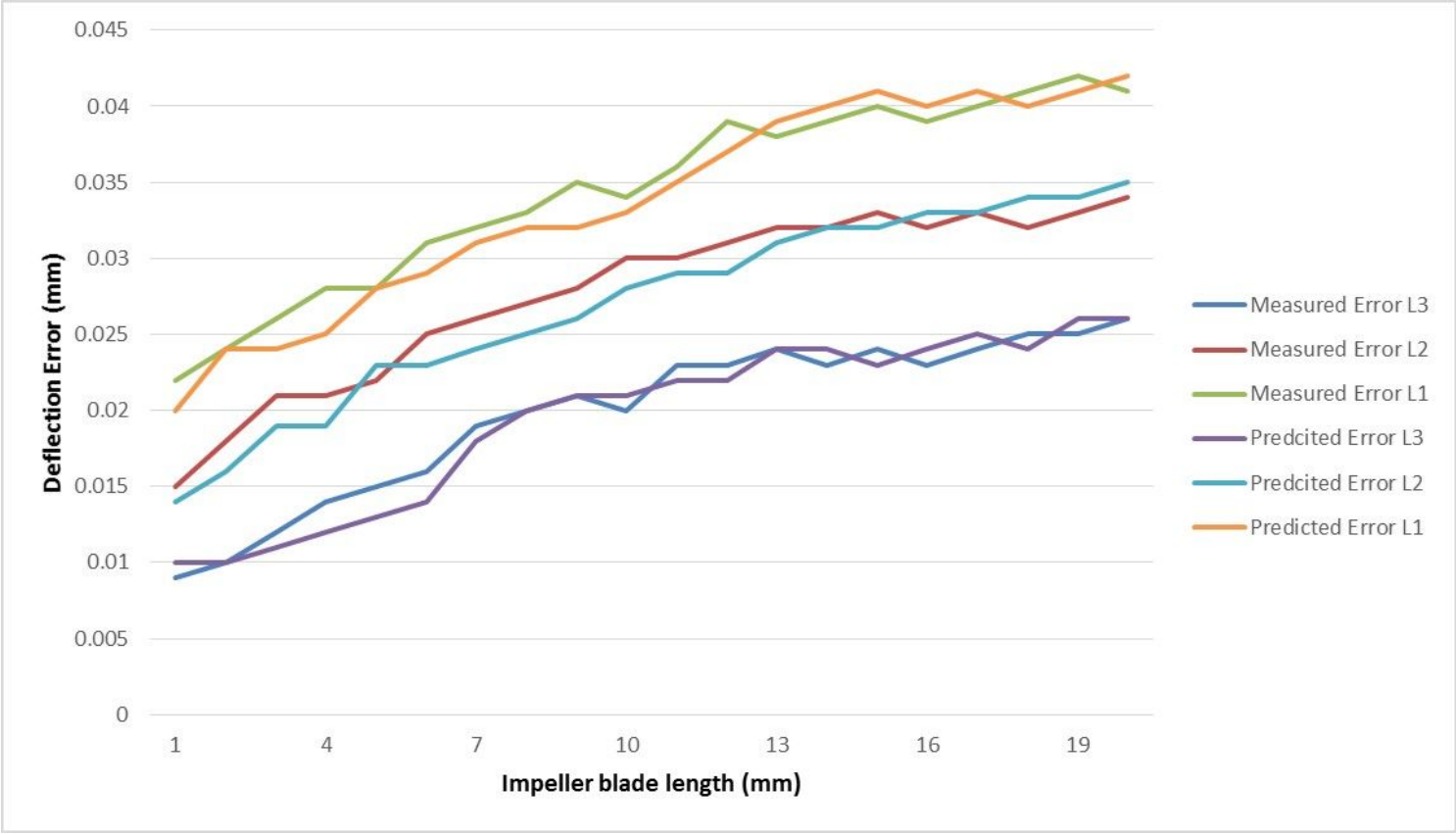

Figure 16

The measured and predicted deflection errors in the machined thin-walled impeller blade.

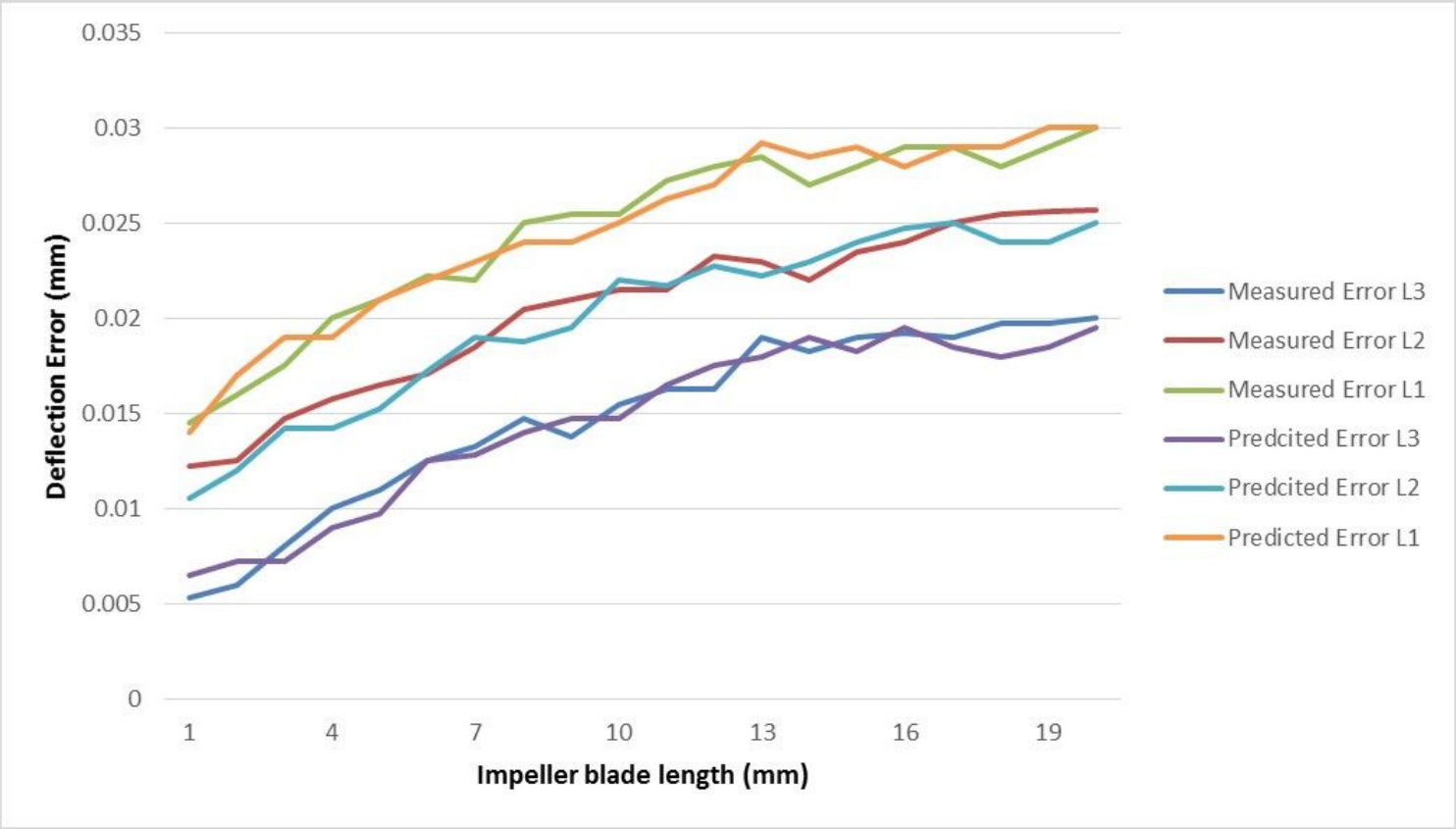

Figure 17

Measured and predicted deflection error of machined thin-walled impeller blade by using optimized machining parameters.